Steel and Composite Structures, *Vol. 18, No. 1 (2015) 29-50*
DOI: http://dx.doi.org/10.12989/scs.2015.18.1.029

Ratcheting behavior of pressurized Z2CND18.12N stainless steel pipe under different control modes

Xiaohui Chen [1,2a], Xu Chen [*2], Gang Chen [2b] and Duomin Li [3c]

[1] *School of Control Engineering, Northeastern University at Qinhuangdao, Qinhuangdao 066004, China*
[2] *School of Chemical Engineering and Technology, Tianjin University, 300072, China*
[3] *Guangdong University of Petrochemical Technology, Maoming 525000, China*

(*Received December 03, 2013, Revised March 10, 2014, Accepted May 22, 2014*)

Abstract. With a quasi-three point bending apparatus, ratcheting deformation is studied experimentally on a pressurized austenitic stainless steel Z2CND18.12N pipe under bending load and vertical displacement control, respectively. The characteristic of ratcheting behavior of straight pipe under both control methods is achieved and compared. The cyclic bending loading and internal pressure influence ratcheting behavior of pressurized straight pipe significantly under loading control and the ratcheting characteristics are also highly associated with the cyclic displacement and internal pressure under displacement control. They all affect not only the saturation of the ratcheting strain but the ratcheting strain rate. In addition, ratcheting simulation is performed by elastic–plastic finite element analysis with ANSYS in which the bilinear model, Chaboche model, Ohno–Wang model and modified Ohno–Wang model are applied. By comparison with the experimental data, it is found that the CJK model gives reasonable simulation. Ratcheting boundaries under two control modes are almost same.

Keywords: ratcheting; cyclic loading; cyclic displacement; loading history; pressure piping

1. Introduction

Pressurized pipes are widely used in nuclear power plants and chemical plants, commonly subjected to cyclic variations of mechanical or thermal secondary stresses. Thus, it is necessary to evaluate whether these components will undergo progressive deformations, so-called ratcheting effect. The ratcheting effect challenges the design of components in nuclear, electric, or chemical industries greatly and the research on the ratcheting has become a hot topic. The ratcheting effect has to be taken into account when designing the components as it has been considered in some standards (such as ASME Code Section III (ASME 2007), KTA (KTA1995) and RCC-MR (RCC-MR 2002)).

A few studies so far addressed the ratcheting simulation of piping components under cyclic bending and internal pressure. Yoshida *et al*. (1984) studied mechanical ratcheting in a carbon

*Corresponding author, Professor, E-mail: xchen@tju.edu.cn
[a] Ph.D., E-mail: chenxh@neuq.edu.cn
[b] Ph.D., E-mail: agang@tju.edu.cn

http://www.techno-press.org/?journal=scs&subpage=8 ISSN: 1229-9367 (Print), 1598-6233 (Online)

steel pipe under combined cyclic axial load and steady internal pressure. It was found that the effects of maximum effective stress, stress ratio and steady stress influenced the biaxial strain accumulation. Guionnet (1989) simulated the ratcheting behavior of austenitic stainless steel (17-12 SPH) tubular specimens in biaxial experiments. Results showed that the Chaboche model reasonably well predicts not only ratcheting but also hysteresis loops and the cyclic hardening curve. Experimental works to study the ratcheting of the straight pipes have been carried out by the EPRI (Ranganath *et al*. 1989, English 1987). Corona and Kyriakides (1991) investigated the degradation and buckling of circular tubes under cyclic bending and external pressure. Rider *et al*. (1994) experimentally examined pressurized pipes for the loading conditions of ± 1% axial strain with hoop stresses of approximately 0, 1/4, 1/2 and 3/4 of the initial uniaxial yield stress. It revealed that both stainless steel and low carbon steel pipes satisfy the proposed ASME ratcheting strain limit of 5% hoop strain after 10 cycles of ± 1% axial strain range for any value of internal pressure. Unlike the ratcheting experiments carried out on the bar specimen in which the uniaxial tensile test method is used, most of the ratcheting experiments of internal pressurized pipes focus on the bending ratcheting behavior, such as cyclic three point bending (Scavuzzo *et al*. 1991), cantilevered bending (Igari *et al*. 1996). Ratcheting data of straight pipe under cyclic bending and steady internal pressure were developed at University of Notre Dame (Corona 1996), Wolters *et al*. (1997) investigated the ratcheting phenomenon of the first wall of a fusion reaction for dominating bending loads, and experimental and theoretical studies on ratcheting were carried out. Krämer *et al*. (1997) researched the ratcheting behavior of austenitic pipes. An extension of the isotropic hardening rule is proposed. Pressurized pipes submitted fluid pressure and bending loads due to thermal expansion, seism and shocks induced from sudden opening and closing of relief valves (Jahanian 1997). Under this kind of loading state, they usually suffer from plastic accumulation namely ratcheting, which could result in reducing fatigue life (Rider *et al*. 1994; Xia *et al*. 1996) or cause failure (Dang-Van and Moumni 2000, Isobe *et al*. 2008) of piping components. Kulkarni *et al*. (2003) studied straight pipe (Sch 80, SA333 Gr. 6 carbon steel) was subjected to a constant internal pressure of 18 MPa and a cyclic bending load. The ovalization of the pipe cross section and local bulging was observed at higher loading. The pipe did not show any shakedown behavior for the given cycles of loading and exhibited continuous ratcheting under the varying loading amplitude. Weiß *et al*. (2004) focused on the design by analysis of welded and non-welded pressure vessel components with respect to combined ratcheting and low cycle fatigue damage mechanisms. An algorithm for the determination of component fatigue curves was proposed. Gao *et al*. (2006) studied experimentally for a pressurized low carbon steel pipe under reversed bending. It revealed that ratcheting strain occurred mainly in the hoop direction. Multi-step bending revealed that the ratcheting rate increased with increasing loading level but reduced or even vanished at a lower bending level imposed after a higher bending level.

On the other hand, ratcheting analysis of pressurized pipes under cyclic bending was performed by elasto-plastic finite element analysis (EPFEA) with elastic perfect plasticity (EPP) model, the bilinear kinematic hardening (BKH) rule (Prager 1956), a combination of BKH and isotropic hardening rule, Chaboche model (Chaboche 1986, 1991), Ohno–Wang model (Ohno and Wang 1993a, b) or the modified Ohno–Wang model (Chen *et al*. 2005). Hassan *et al*. (1998) improved the ratcheting analysis of a piping component by incorporating an improved cyclic plasticity model, which was composed of the Armstrong-Frederick hardening rule and the Drucker–Palgen plastic modulus equation, into an ANSYS material model subroutine. Kobayashi *et al*. (2003), Kobayashi and Ohno (2002), Kang *et al*. (2002), Postberg and Weiß (2007) and Gao (2005) incorporated the Ohno–Wang model or the modified Ohno–Wang model into ANSYS or

ABAQUS for improving ratcheting analysis. (Kulkarni *et al*. 2004) experimentally studied the ratcheting of a straight pipe with a 4-point bending apparatus and analyzed its ratcheting with the Chaboche model in ANSYS. DeGrassi *et al*. (2003) performed nonlinear time history analysis on piping system and simulated the results through plasticity model with bilinear, multilinear and Chaboche kinematic hardening rules. The authors showed that the best simulation can be obtained with the Chaboche plasticity model in ANSYS. Rahman (2006) and Rahman *et al*. (2008) investigated various numerical challenges occurred during the model implementation process. He evaluates the performance of the constitutive models in simulating the global and local ratcheting responses of straight pipe subjected to internal pressure and cyclic bending. Zakavi *et al*. (2010) studied the ratcheting behavior of pressurized plain pipework subjected to cyclic bending moment with the combined hardening model. The finite element results were compared with those obtained from experimental set-up. The results showed that the initial rate of ratcheting was large and then it decreased with the increasing cycles. So far, most of the ratcheting experiments of internal pressurized pipes have been carried out under loading control while only a few scholars studied the characteristic of the bending ratcheting behavior conducted under displacement control (Vishnuvardhan *et al*. 2010). Since the thermal stress could cause a certain bending deformation and the in-service pipes are always constrained by the structure which makes the maximum bending deformation constant, it is necessary to investigate the bending ratcheting behavior of the internal pressurized pipes under displacement control.

So far, BKH model, a combination of BKH and isotropic hardening rule and Chaboche model are available in ANSYS software. The advanced plasticity models with modified Chaboche, Ohno-Wang, Abdel Karim-Ohno and modified Ohno-Wang kinematic hardening rules were customized with ANSYS through the option of user programmable features. Thus, this study will evaluate several plasticity models through finite element simulation of experimental data and develop a numerical tool for structural ratcheting simulation.

2. Experiments study of ratcheting

2.1 Pipe material and specification

The pipe material used in this study is austenitic stainless steel Z2CND18.12N (in French materials designation). The main chemical compositions of the material are shown in Table 1. Yield strength of the material is 388 MPa and Young's modulus is 195 GPa at room temperature.

The pipe specimens were straight pipes with dimensions of 76 mm outside diameter, 4.5 mm thickness and 1.2 m length to the required length, and welded with pipe ends. Annealing was done after verification of welds by X-ray.

2.2 Experimental apparatus and testing system

Table 1 Main chemical composition of Z2CND18.12N stainless steel (wt. %)

Specification	Chemical composition (%)											
	C	Cr	Ni	Si	Mn	S	P	B	Mo	Cu	Co	N
$\varphi 76 \times 4$	0.025	17.517	12.073	0.430	1.221	0.003	0.021	0.001	2.388	0.075	0.035	0.070

The quasi-three point bending apparatus is shown in Fig. 1, in which dimensions are in millimeter. The specimen is supported on the lower loading beam, which is stiff enough, through supporting ears, clip boards, pins, bolts and nuts. The upper loading beam is also stiff enough and connected to the specimen with clip boards, pins, bolts and nuts. Both the loading bar screwed into the upper loading beam and the loading block welded on the lower loading beam is clipped in the clamp head of the test machine. Cyclic pull–push of the test machine bends the specimen reversely. Internal pressure is applied with another branch of the pressure system. Thin walled pipes under internal pressure are in bi-axial stresses states, and axial bending stresses from the pull-push action on the specimen are cyclically applied to achieve non-proportional multi-axial loading. Tests are conducted on a closed-loop servo-hydraulic tension-compression testing machine. The set-up of the apparatus is shown in Fig. 2.

In order to record the ratcheting strains, biaxial strain gauges are adhered on the specimen aligned to the axial and hoop direction. These gauges are assigned to the positions presented in

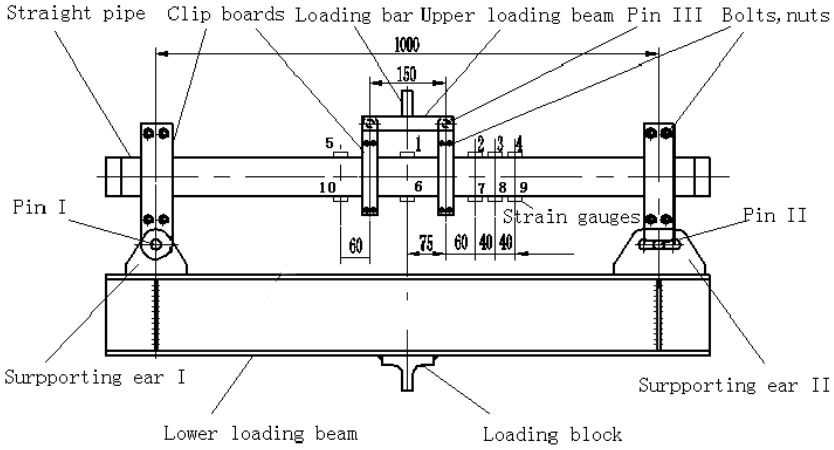

Fig. 1 Sketch of the quasi-three point bending apparatus and gauge positions

Fig. 2 Setup of experiment apparatus

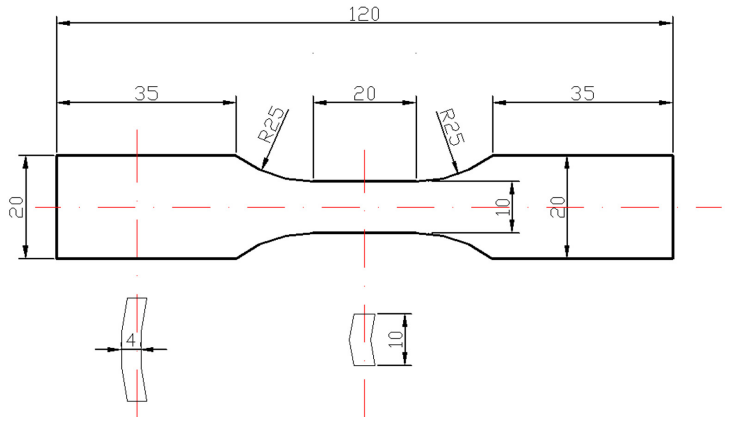

Fig. 3 Specimen geometry and dimensions (units: mm)

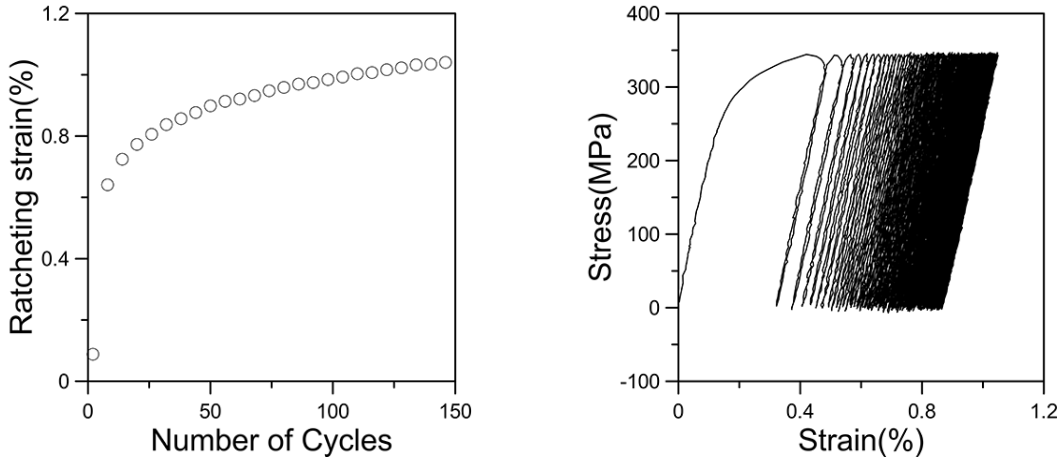

(a) Ratcheting strain (b) Strain-stress curve

Fig. 4 Uniaxial ratcheting data

Fig. 1. The values of loading, strain, and time are simultaneously recorded by computer-controlled system of data acquisition. Plate-shape specimens (Fig. 3) were cut from the straight pipes used for the ratcheting study. They were flattened and machined into the desired shape, then annealed and ground to the final dimensions of 10 mm width, 3.8 mm thickness, and 25 mm length, in the gauge section. Extensometer with gage length of 12.5 mm was attached on specimen to measure axial strain.

3. Experimental results and analysis

3.1 Monotonic tensile test and uniaxial ratcheting test

The mechanical properties of austenitic stainless steel Z2CND18.12 N are determined by the

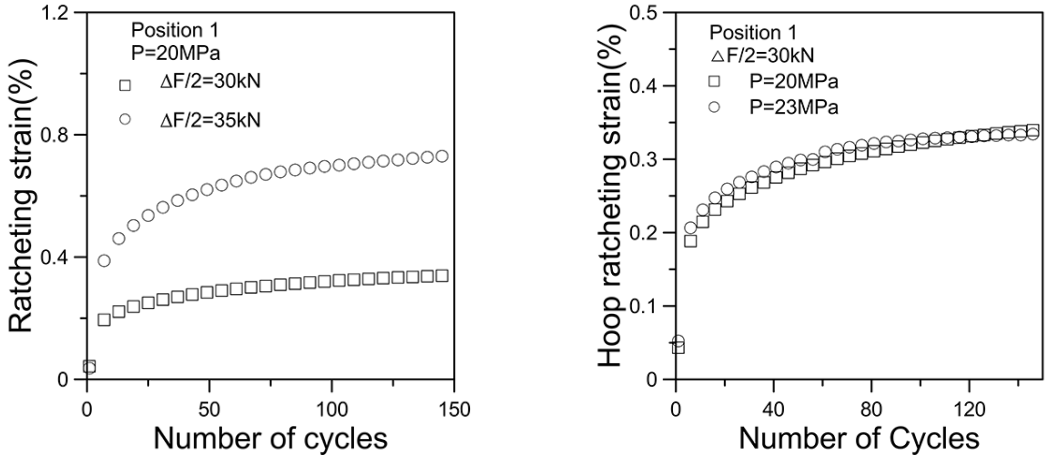

(a) P = 20 MPa, $\Delta F/2$ = 30, 35 kN (b) $\Delta F/2$ = 30 kN, P = 20, 23 MPa

Fig. 5 Ratcheting strain of straight pipe with internal pressure and bending load

monotonic stress-strain curve. Young's modulus for elasticity E = 195 GPa, 0.2% proof stress Sy = 388 MPa.

Uniaxial ratcheting testing was conducted with a loading of stress ranges 150 MPa under a constant mean stress of 150 MPa. The ratcheting strains are given in Fig. 4. This indicates that ratcheting strains increased with the number of cycles.

3.2 Ratcheting of straight pipe under loading control

The hoop ratcheting strains are given in Fig. 5(a) for tests of 20 MPa internal pressure under various bending loads (30 kN and 35 kN) from individual specimens. It is notable that ratcheting rates increased with bending load under constant internal pressure.

Fig. 5(b) shows the hoop ratcheting strains of straight pipe for tests of 30 kN bending load under various internal pressures (20 MPa and 23 MPa). Ratcheting strain rates increase with internal pressure under constant bending load. It is seen from Fig. 6 that hoop ratcheting strain rate grow with an increase of the bending loading level at the same internal pressure or with an increase of internal pressure at the same bending load, but the influence of internal pressure is relatively smaller than that of bending load.

3.3 Ratcheting of straight pipe under displacement control

The hoop ratcheting strains of straight pipe under constant internal pressures of 17.5 MPa and a vertical displacement of 5 mm and 6 mm are shown in Fig. 6(a). Ratcheting rates increase with vertical displacement under constant internal pressure.

The hoop ratcheting strains are given in Fig. 6(b) for tests of 6 mm vertical displacement under various internal pressures (17.5 MPa and 20 MPa) from individual specimens. Ratcheting rates increase with internal pressure under constant bending load. It is seen from Fig. 6 that hoop ratcheting strain rate grow with an increase of the vertical displacement level at the same internal pressure or with an increase of internal pressure at the same vertical displacement, but the

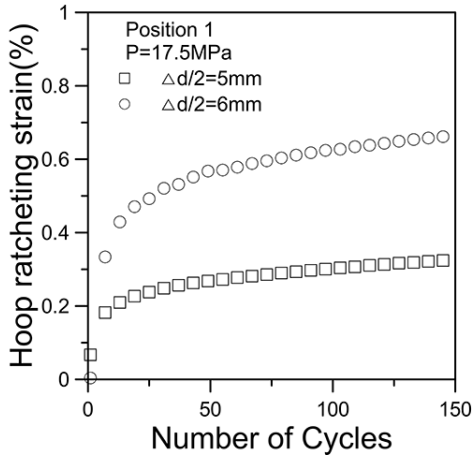

(a) P = 17.5 MPa, $\Delta d/2$ = 5 mm and 6 mm

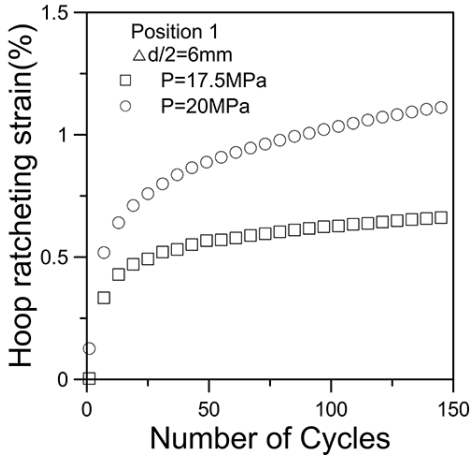

(b) $\Delta d/2$ = 6 mm, P = 17.5 MPa and 20 MPa

Fig. 6 Ratcheting strain of straight pipe with internal pressure and cyclic displacement

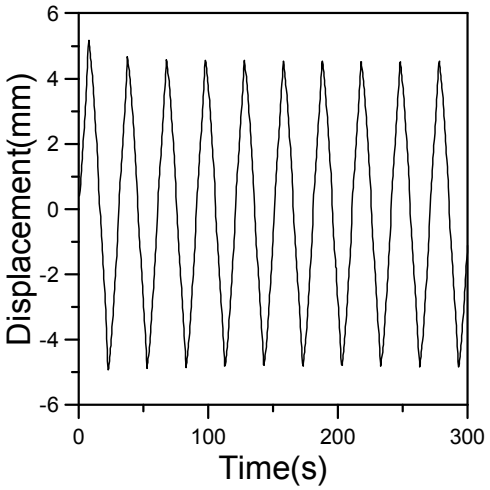

(a) The changes of the displacement in the first 10 cycles

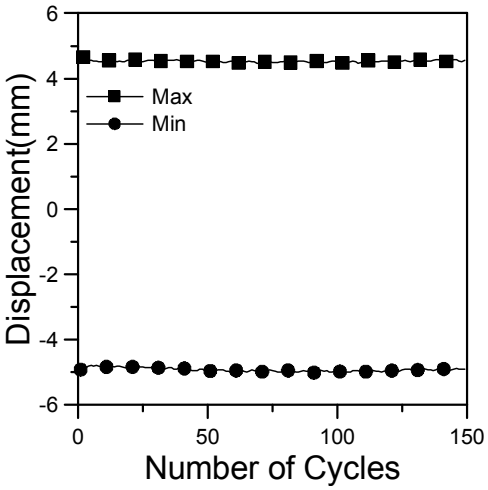

(b) Displacement maximum

Fig. 7 Displacement in each cycle versus the number of cycles under loading control

influence of vertical displacement is relatively greater than that of internal pressure.

3.4 Comparison of the bending ratcheting behaviors under different control modes

Fig. 7(a) indicates the changes of the displacement of straight pipe under the bending load of 30 kN and constant internal pressure of 20 MPa. The maximum and minimum displacement each cycle versus the number of cycles is shown in Fig. 7(b). It can be seen clearly that the displacement amplitude in the first cycle is much larger than that in the following cycles. The internal pressurized pipe shows the quickly hardening trend in the first cycle under the bending loading

control. Moreover, the maximum and minimum displacement is close to 5 mm and -5 mm respectively after the first cycle. Therefore, the test of internal pressurized pipe under displacement control is conducted under the controlled cyclic displacement of ± 5 mm and the constant internal pressure.

The bending loading response of straight pipe under the vertical displacement of 5 mm and constant internal pressure of 20 MPa under displacement control is plotted in Fig. 8. As can be seen in Fig. 8, the bending loading amplitude in the first cycle is much larger than that in the following cycles. The internal pressurized pipe also shows the quickly hardening trend in the first cycle under the displacement control, which is highly similar with the trend under loading control. Moreover, the maximum and minimum loading is around 30 kN and -30 kN respectively after the first cycle.

Comparing the ratcheting strain at each position under different control modes, it is obvious that the ratcheting strain under the displacement control is similar with that under the loading control, though the ratcheting strain under the displacement control at Position 6 and Position 7 is a bit larger than that under the loading control. The difference at Position 6 and Position 7 is because the bending loading under displacement control was a bit higher than that of straight pipe under the bending load of 30 kN and constant internal pressure of 20 MPa under loading control. Moreover, it is obvious that the displacement response is almost the same with that in the displacement control after the first cycle according to Fig. 7(a) and the bending loading response under the displacement control is also the same with that in the loading control after the first cycle as shown in Fig. 8(a). Therefore, it can be concluded that the control mode influences the characteristics of the bending ratcheting behavior slightly and there may be only some differences in first cycle of the ratcheting strain under different control modes. In addition, the ratcheting behavior under loading control could be used to forecast the characteristics of the ratcheting behavior under displacement control and vice versa.

Then, the ratcheting strain at each position under different control modes is obtained and compared in Fig. 9. Fig. 10 shows the relationship between the bending moment and the hoop ratcheting strain at Position 1.

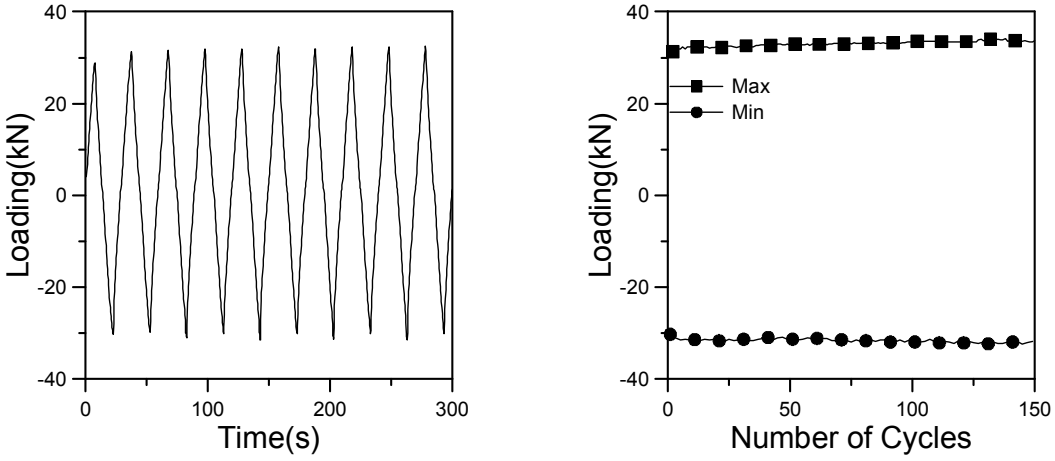

(a) The changes of the loading in the first 10 cycles (b) Loading maximum

Fig. 8 Bending loading versus the number of cycles under displacement control

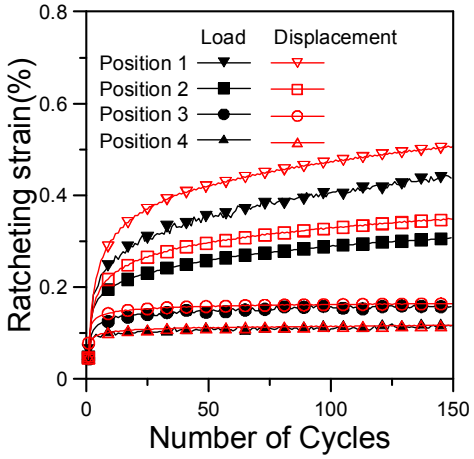

Fig. 9 Ratcheting strain at each position under different control modes

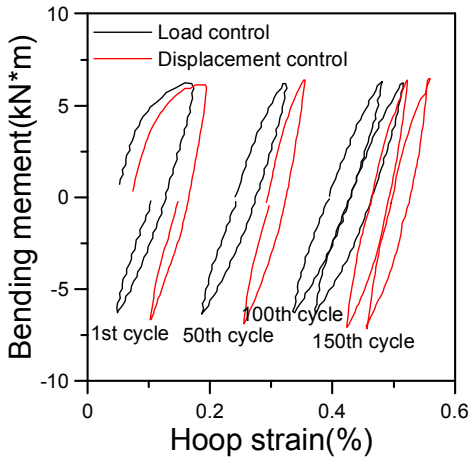

Fig. 10 Bending moment versus hoop strain at Position 1

3.5 Ratcheting boundary determination

Fig. 9 shows the hoop ratcheting strain versus number of cycles at various positions under loading control and displacement control. It reveals that hoop ratcheting strain rate at different positions is different under different control modes. The quasi-three point bending apparatus provides different bending moments at different positions. However, the ratcheting boundary for the applied internal pressure can be determined by the ratcheting rate at various positions at different bending loads. Ratcheting boundary is determined by the regression technique (Yahiaoui and Moffat 1996). The ratcheting strain rates at various positions are plotted versus bending loads as shown in Fig. 11. It is found to be 22.788 kN for 20 MPa internal pressure under load control (Fig. 11(a)) and 20.17 kN for 20 MPa internal pressure under displacement control (Fig. 11(c)). The ratcheting boundary determined in this way under load and displacement control is shown in Figs. 11(b) and (d), respectively.

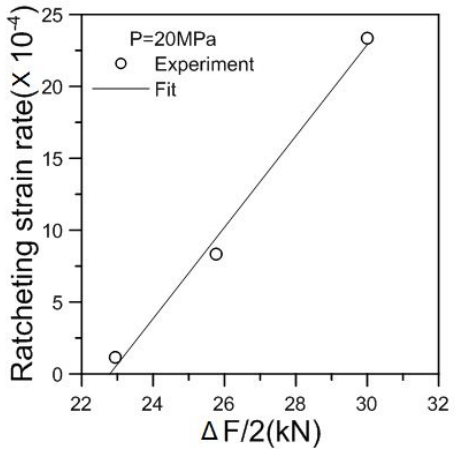

(a) Ratcheting strain rate versus bending moment

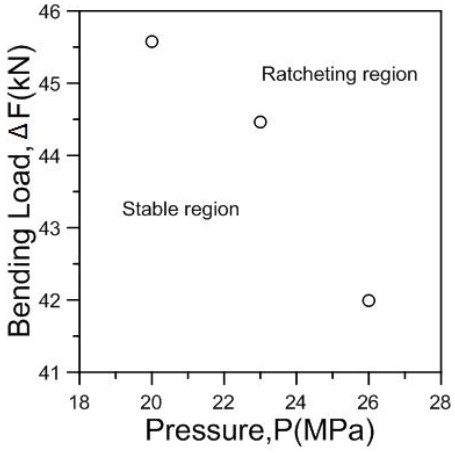

(b) Ratcheting boundary under loading control

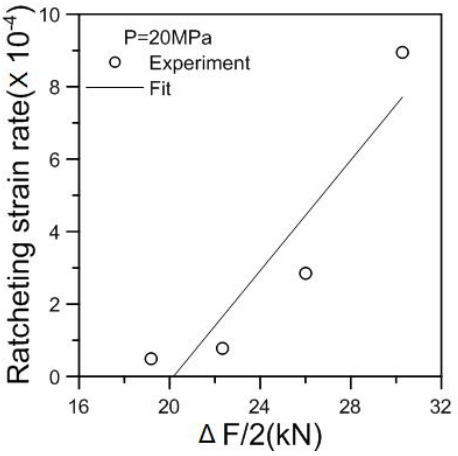

(c) Ratcheting strain rate versus bending moment

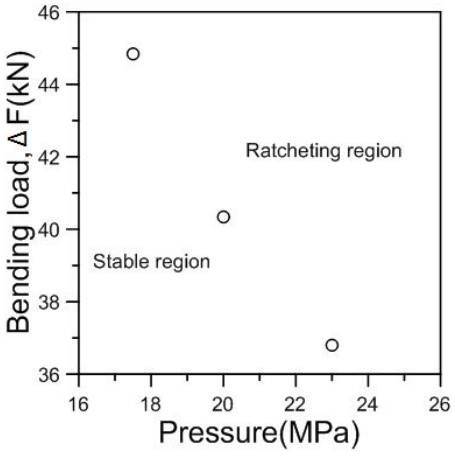

(d) Ratcheting boundary under displacement control

Fig. 11 Determination of ratcheting boundary under load and displacement control

4. Ratcheting strain simulation

4.1 Ratcheting strain simulation

Ratcheting strain simulations are based on the following rate independent plasticity model.
(i) von Mises yield surface

$$f(\sigma-\alpha)=\left[\frac{3}{2}(s-\alpha):(s-\alpha)\right]^{1/2}=\sigma_0 \tag{1}$$

(ii) flow rule

$$d\varepsilon^p=\frac{1}{H}\left\langle\frac{\partial f}{\partial\sigma}:d\sigma\right\rangle\frac{\partial f}{\partial\sigma} \tag{2}$$

Here, σ is the stress tensor, ε^p is the plastic strain tensor, s is the deviatoric stress tensor, α is the current centre of the yield surface in deviatoric stress space, σ_0 is the size of the yield surface (constant for a cyclically stable material), and H is the plastic modulus. Also, $\langle\rangle$ indicates the MacCauley bracket and the inner product $a : b = a_{ij}b_{ij}$.

(iii) the kinematic hardening rule is given by

$$d\alpha = g(\sigma, \varepsilon^p, \alpha, d\sigma\sigma, \varepsilon^p, etc.) \tag{3}$$

The kinematic hardening rule dictates the evolution of the yield surface during a plastic loading increment by translation in stress space only. In this paper the modified Ohno–Wang models are used for ratcheting simulation.

4.2 Constitutive model

4.2.1 The bilinear model

Linear kinematic hardening rule was first proposed by Prager (1956) as

$$d\alpha = Cd\varepsilon^p \tag{4}$$

The parameters of the bilinear model are determined by approximating the hysteresis stress-strain loop as shown in Fig. 12. The model parameters include elastic modulus, E = 195000 MPa, yield stress, σ_0 = 388 MPa and plastic modulus, E_p = 1712 MPa.

4.2.2 Chaboche model

Chaboche and his co-workers (Chaboche 1986, 1991) proposed that several Armstrong and Frederick type rules were superimposed as

$$d\alpha = \sum_{i=1}^{M} d\alpha_i = \sum_{i=1}^{m} \left(\frac{2}{3} C_i d\varepsilon^p - \gamma_i \alpha_i dp \right) \tag{5}$$

where α_i is the i-th component of deviatoric back stress α, C_i, γ_i are material constants, which can

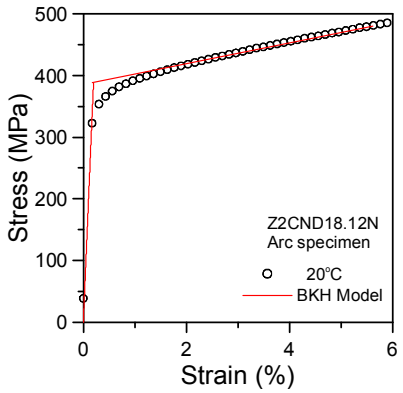

Fig. 12 Bilinear model parameter determination

be determined by the uniaxial test. The parameter determination scheme has been discussed by Bari and Hassan (Bari and Hassan 2000) in detail. For Z2CND18.12N stainless steel used in this study, six items are adopted and the values of the parameters are:

σ_0 = 100 MPa; C_i = 4.0 × 10^6, 1.5 × 10^5, 2.5 × 10^3; γ_i = 4.0 × 10^4, 0.83 × 10^3, 4.5, which are determined through simulating the composed hysteresis curve and uniaxial ratcheting response (Fig. 13).

4.2.3 Ohno-Wang model

Ohno and Wang (1993a) proposed the kinematic hardening rule as

$$d\alpha = \sum_{i=1}^{M} d\alpha_i \tag{6}$$

$$d\alpha_i = \gamma_i \left[\frac{2}{3} r_i d\varepsilon^p - \left(\frac{\bar{\alpha}_i}{r_i} \right)^{m_i} \left\langle d\varepsilon^p : \frac{\alpha_i}{\bar{\alpha}_i} \right\rangle \alpha_i \right] \tag{7}$$

where, γ_i, r_i and m_i are model parameters and M is the number of linear segments required for multilinear representation of uniaxial stress-strain curve. The parameters of the Ohno-Wang plasticity model are: σ_0 = 100 MPa; m_i = 6; r_i = 40, 107, 60, 18, 60, 110;

γ_i = 8000, 4000, 2000, 1500, 150, 20; which are determined through simulating the composed hysteresis curve and uniaxial ratcheting response (Fig. 14).

4.2.4 Chen-Jiao-Kim model (CJK model)

Chen, Jiao, and Kim (Chen *et al*. 2005) proposed a modified Ohno-Wang kinematic hardening rule in which a multiaxial parameter χ_i was introduced. The model is shown as

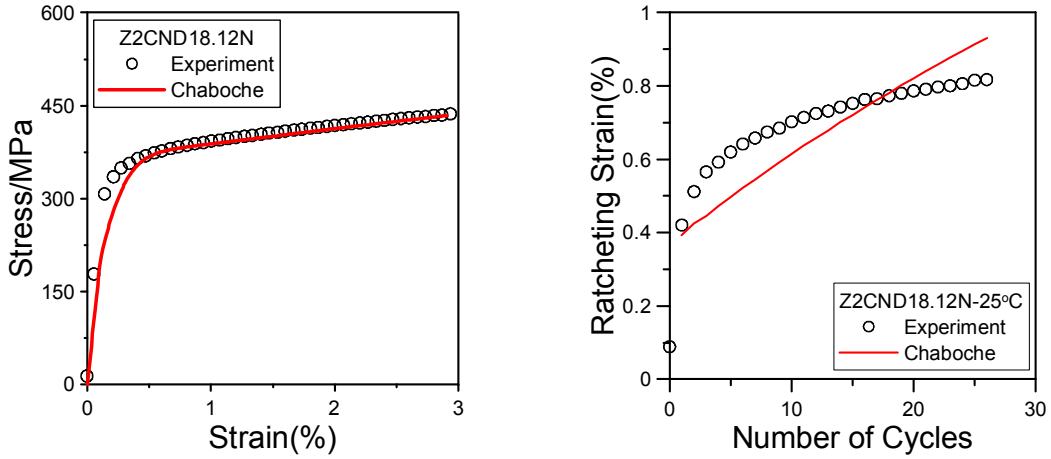

(a) Hysteresis loop representation (b) Unaxial ratcheting simulation

Fig. 13 Model parameter determination and material response simulations with Chaboche model

$$\alpha = \sum_{i=1}^{M} \alpha_i \tag{9}$$

$$d\alpha_i = \gamma_i \left[\frac{2}{3} r_i d\varepsilon^p - \left\langle n' : \frac{\alpha_i}{\bar{\alpha}_i} \right\rangle^{\chi_i} \left(\frac{\bar{\alpha}_i}{r_i} \right)^{m_i} \alpha_i \left\langle d\varepsilon^p : \frac{\alpha_i}{\bar{\alpha}_i} \right\rangle \right] \tag{10}$$

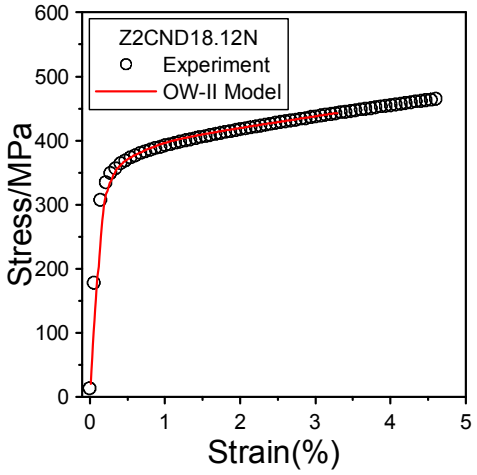

(a) Hysteresis loop representation

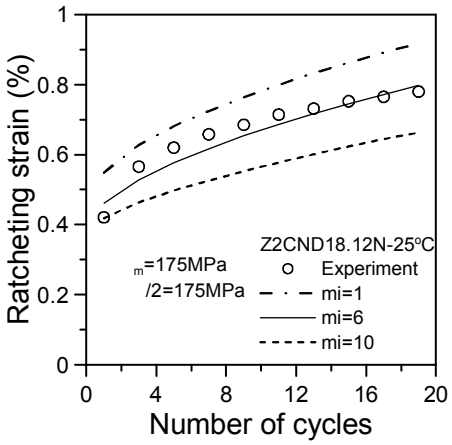

(b) Unaxial ratcheting simulation

Fig. 14 Model parameter determination and material response simulations with Ohno-Wang model

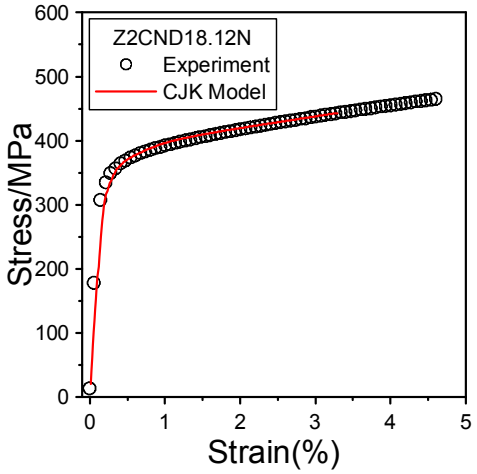

(a) Hysteresis loop representation

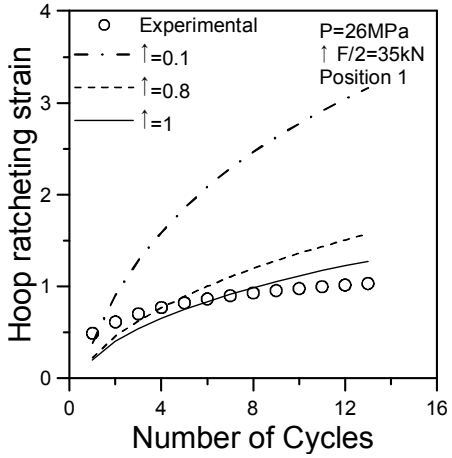

(b) Ratcheting prediction of straight pipe

Fig. 15 Model parameter determination and material response simulations with CJK model

where $n' = \frac{d\varepsilon^p}{dp} = \frac{3}{2\sigma_0}(s-\alpha)$, $\overline{\alpha}_i$ is the magnitude of α_i, $\overline{\alpha}_i = \sqrt{3/2\alpha_i : \alpha_i}$, and χ_i is multiaxial parameter. The parameters of the modified Ohno-Wang (Chen *et al*. 2005) plasticity model are: σ_0 = 100 MPa; m_i = 6; χ_i = 1; γ_i = 8000, 4000, 2000, 1500, 150, 20; r_i = 40, 107, 60, 18, 60, 110; which are determined through simulating the composed hysteresis curve and uniaxial ratcheting response (Fig. 15(a)). The hoop ratcheting strain at position 1 of the specimen is obtained by elastic-plastic finite element analysis with ANSYS, in which the CJK model is applied by user programming is shown in Fig. 15(b).

4.3 Analysis and Discussion

4.3.1 Ratcheting effect of straight pipe under loading control

In this paper, Bilinear, Chaboche, Ohno-Wang and CJK model are used for simulating the ratcheting strain of straight pipe. The Finite Element Analysis model is shown in Fig. 16, in which only a quarter of the structure is included due to symmetry. Six hundred shell43 elements are used to mesh the pipe and 121 shell43 elements are used to mesh the end plate. In addition to the symmetric displacement constraints, displacement in the *y*-direction is applied to the central point of the end plate. Internal pressure is applied to the inside surface of the pipe and end plate. Reversed bending load or cyclic vertical displacement in the *y*-direction is distributed to nodes at the position corresponding to the central line of the clip board of the upper loading beam.

The ratcheting strain simulation is first discussed with the test results for 20 MPa internal pressure and 30 kN bending load. Comparison of experimental results with simulating results at position 1 is shown in Fig. 17. It is found that prediction results of CJK model are better than other models. Bilinear model shows prediction for ratcheting strain of straight pipe due to the high yield stress parameter. Chaboche model shows over prediction for ratcheting strain of straight pipe. Ohno-Wang model shows lower prediction than Chaboche model but still over prediction for the experiments. Prediction results of different positions with CJK model are given in Fig. 18. It is seen from Fig. 18 that ratcheting strains of straight pipe decrease from the centre of pipe to two ends.

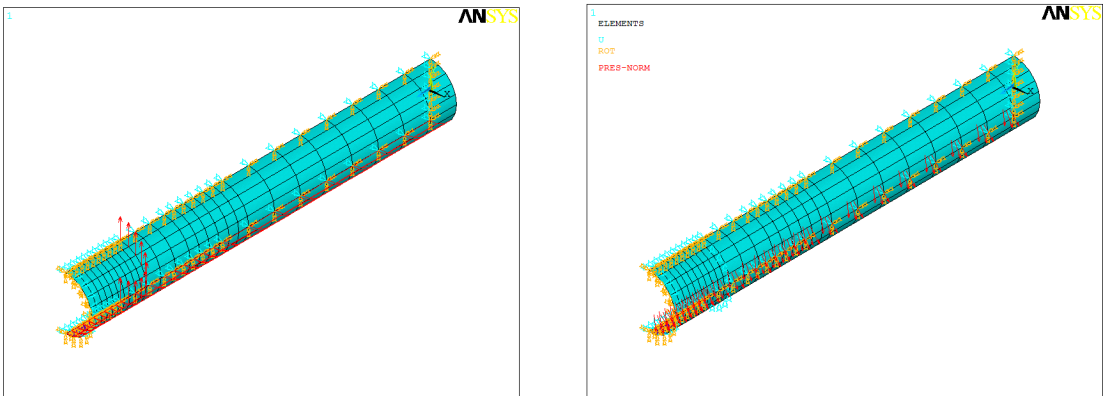

(a) Cyclic bending loading (b) Cyclic displacement

Fig. 16 Finite element analysis model

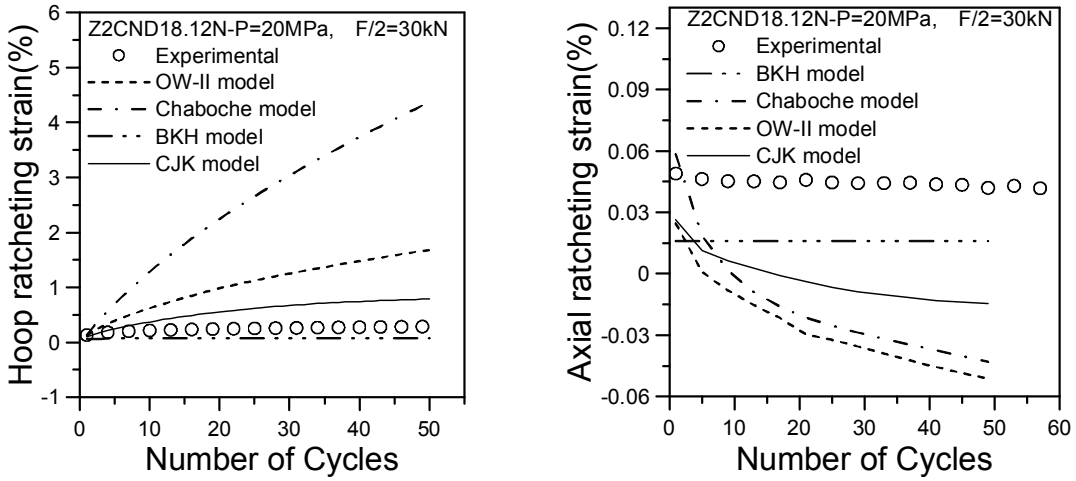

(a) Hoop ratcheting strain (b) Axial ratcheting strain BKH is good

Fig. 17 Comparison of experimental and predicted ratcheting response by constitutive model

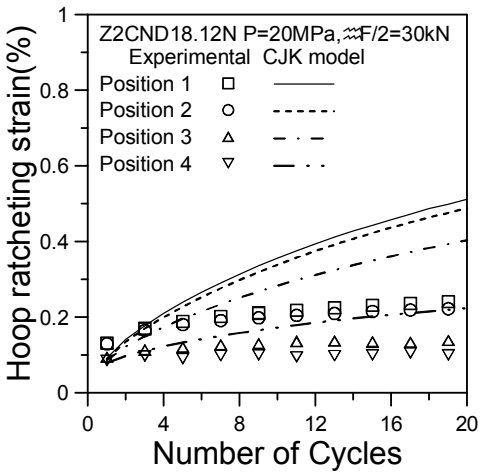

Fig. 18 Comparison of experimental and predicted ratcheting response by CJK model

Comparison of Ratcheting strain of straight pipe under internal pressure of 26 MPa and bending load of 30 kN and 35 kN respectively is shown in Fig. 19(a). It shows that ratcheting strain rate increases with increasing of bending load under the same internal pressure. Fig. 19(b) gives comparison of ratcheting strain of straight pipe under bending load of 35 kN and internal pressure of 20 MPa and 26 MPa respectively. Under the same bending load the ratcheting strain rate increases with increasing of internal pressure as shown in Fig. 19(b).

4.3.2 Ratcheting effect of straight pipe under displacement control

Fig. 20 shows the comparison of ratcheting strain of straight pipe under internal pressure of 20 MPa and vertical displacement of 6 mm at position 1. It is found that prediction results of CJK

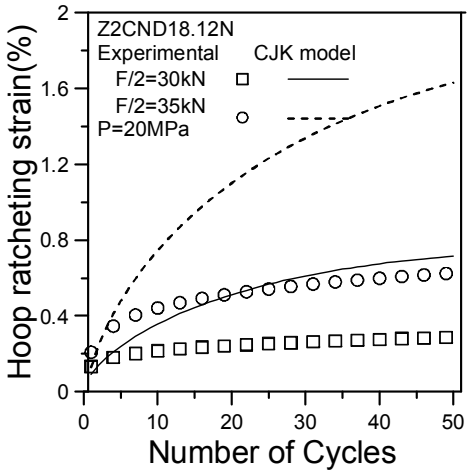

(a) Various bending loading with constant internal pressure

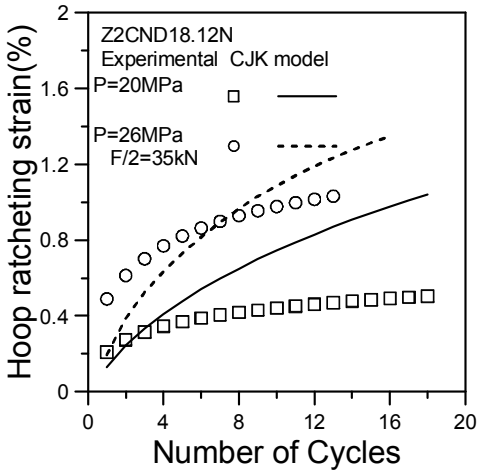

(b) Various internal pressures with constant bending loading

Fig. 19 Comparison of experimental and predicted ratcheting strain by CJK model

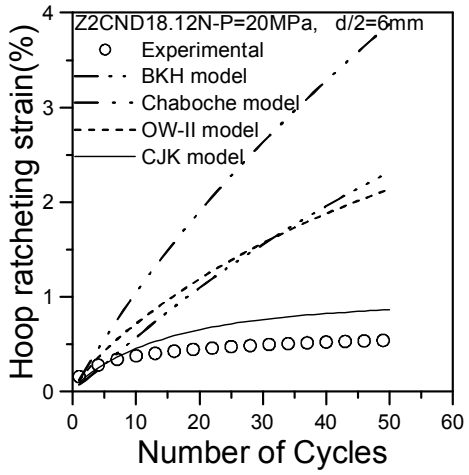

(a) Hoop ratcheting strain

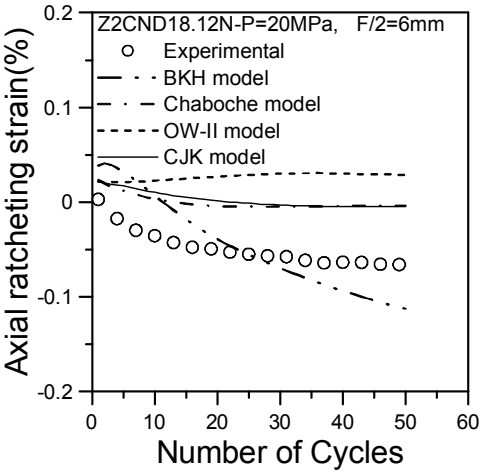

(b) Axial ratcheting strain

Fig. 20 Comparison of experimental and predicted ratcheting response by constitutive model

model are better than that of other models. Bilinear model, Chaboche model, Ohno-Wang model shows over prediction for the experiments. Ratcheting strains of straight pipe decrease from the centre of pipe to two ends are given in Fig. 21.

Fig. 22(a) shows ratcheting strain comparison of straight pipe under internal pressure of 20 MPa and vertical displacement of 5 mm and 6 mm respectively. It shows that ratcheting strain rate increases with increasing of bending load under the same internal pressure. Comparison of ratcheting strain of straight pipe under vertical displacement of 6 mm and internal pressure of 17.5 MPa and 20 MPa is given in Fig. 22(b), respectively. Under the same vertical displacement the

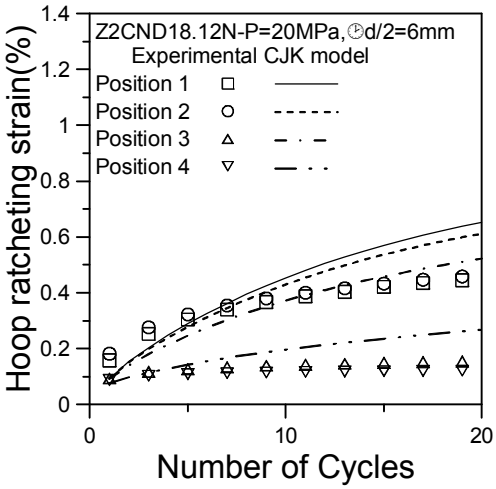

Fig. 21 Comparison of experimental and predicted ratcheting response by CJK model

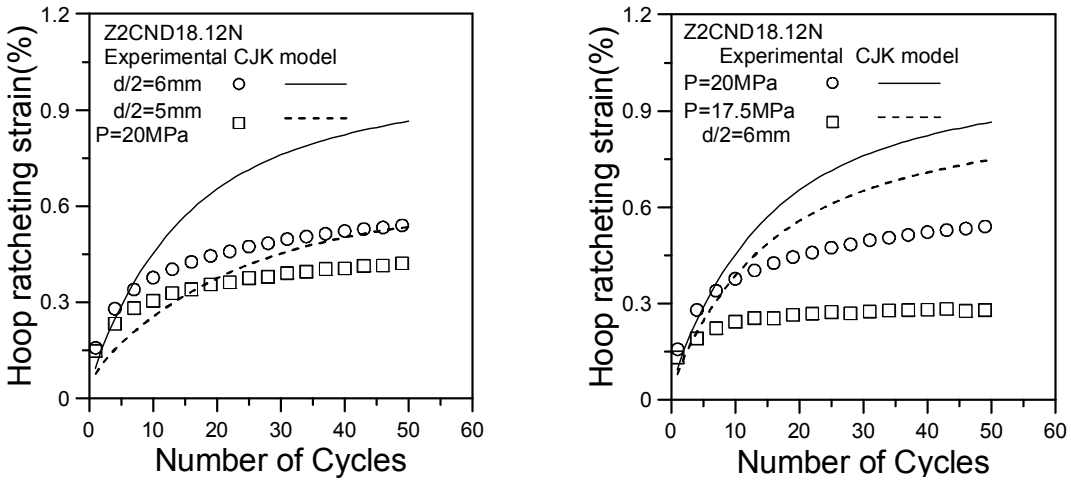

(a) Various vertical displacement with constant internal pressure

(b) Various internal pressure with constant vertical displacement

Fig. 22 Comparison of experimental and predicted ratcheting response by CJK model

ratcheting strain rate increases with increasing of internal pressure as shown in Fig. 22(b).

4.4 Comparison of the bending ratcheting behaviors under different control modes

Fig. 23(a) indicates the changes of the displacement of straight pipe under the bending load of 30 kN and constant internal pressure of 20 MPa. The maximum and minimum displacement of each cycle for straight pipe versus the number of cycles is shown in Fig. 23(b). It can be seen clearly that the displacement amplitude in the first cycle is slightly larger than that in the following cycles. The internal pressurized pipe shows the quickly hardening trend in the first cycle under the

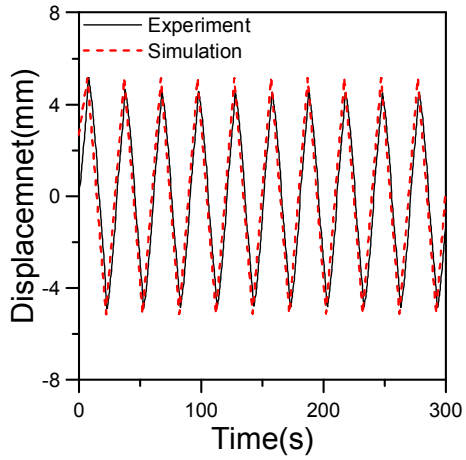

(a) Displacement profile in the first 10 cycles

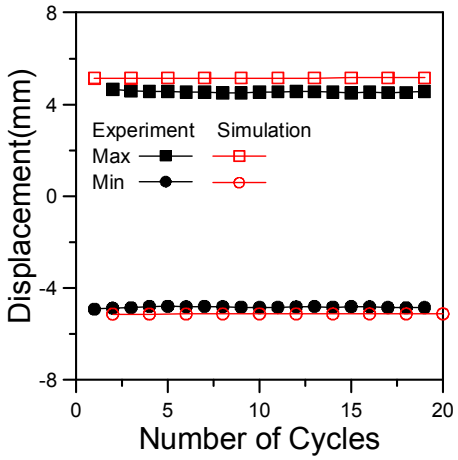

(b) The maximum and minimum displacement

Fig. 23 Displacement in each cycle versus the number of cycles under loading control

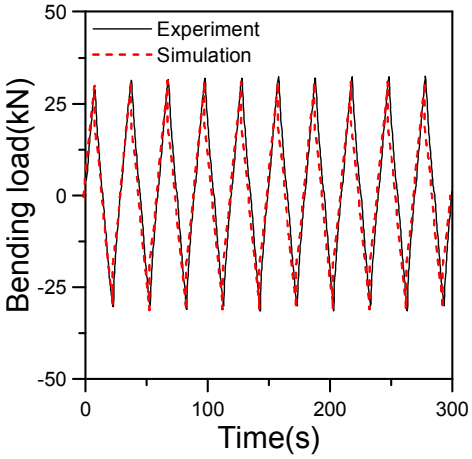

(a) The changes of the displacement in the first 10 cycles

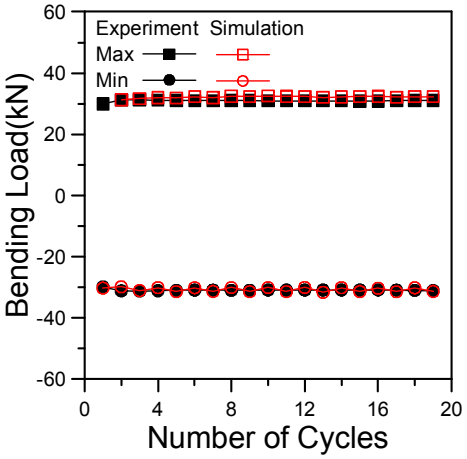

(b) The maximum and minimum bending load

Fig. 24 Bending load in each cycle versus the number of cycles under displacement control

bending loading control. Moreover, the maximum and minimum displacement is around 5.16 mm and -5.12 mm respectively after the first cycle. In general, the results of simulation are higher than those of experiments. Therefore, the test of internal pressurized pipe under displacement control is conducted under the controlled cyclic displacement of ± 5 mm and the constant internal pressure 20 MPa.

The bending loading response of straight pipe under the vertical displacement of 5 mm and constant internal pressure of 20 MPa under displacement control is plotted in Fig. 24. As can be seen in Fig. 24, the bending loading amplitude in the first cycle is much smaller than that in the following cycles. Moreover, the maximum and minimum loading is around 30 kN and -30 kN

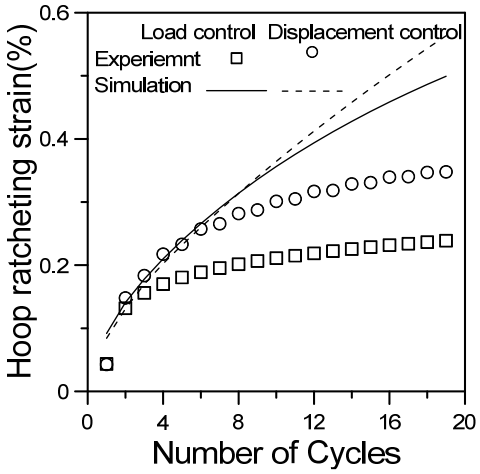

Fig. 25 Ratcheting strain under different control modes

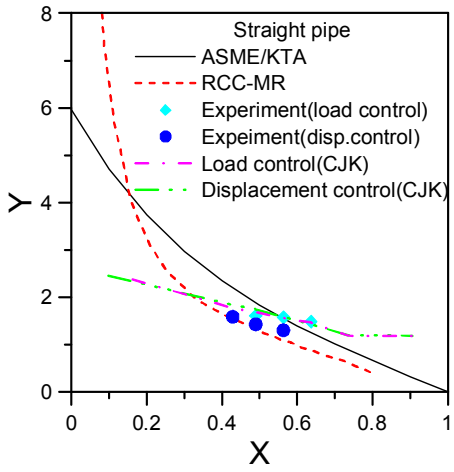

Fig. 26 Ratcheting boundary under different control modes

respectively after the first cycle. The results of simulation by CJK model match well with experimental data.

Then, the ratcheting strain at position 1 under different control modes is obtained and compared in Fig. 25. Comparing the ratcheting strain of experiment at position 1 with that of simulation, it is obvious that the ratcheting strain under the displacement control is similar with that under the loading control, though the ratcheting strain under the displacement control at Position 1 is a bit larger than that under the loading control. The difference at Position 1 is because the bending loading under displacement control is a bit higher than that of straight pipe under the bending load of 30 kN and constant internal pressure of 20 MPa under loading control. Moreover, it is obvious that the displacement response is almost the same with that in the displacement control after the first cycle and the bending loading response under the displacement control is also the same with that in the loading control after the first cycle. Therefore, it can be concluded that the control mode

influences the characteristics of the bending ratcheting behavior slightly and there may be only some differences in first cycle of the ratcheting strain under different control modes. In addition, the ratcheting behavior under loading control could be used to forecast the characteristics of the ratcheting behavior under displacement control and vice versa. The internal pressurized pipe shows the quickly hardening trend in the first cycle under loading and displacement control (Yu *et al*. 2011).

4.5 Ratcheting boundary determination

Evaluating variations in plastic strain increments of C-TDF methods is applied to verify shakedown (Asada *et al*. 2002). Comparison of experiment and simulation with ASME and RCC is shown in Fig. 26. It shows that ratcheting boundary under load control and displacement control is almost same in the experiment. In addition, Ratcheting boundary of the simulations has very good correlations with the experiments.

5. Conclusions

With the quasi-three point bending apparatus, ratcheting strain of pressurized straight Z2CND18.12N stainless steel pipe under loading and displacement control were investigated experimentally. The impact of the control mode on the bending ratcheting strain was discussed. The characteristics of the bending ratcheting strain under different internal pressures and different controlled cyclic displacement or loading were compared. Moreover, the influence of the bending history on the bending ratcheting behavior was studied. Accumulation of the strain was observed at each position both in the hoop as well as axial directions of the internal pressurized pipes under displacement and loading control. However, the ratcheting strain occurs mainly in the hoop direction and the ratcheting strain rate is also higher in the hoop direction. The internal pressure and the controlled cyclic displacement or bending loading influences the characteristics of the bending ratcheting behavior. Higher level of internal pressure or displacement (or bending loading) could result in the larger ratcheting strain and the higher ratcheting strain rate. The control mode influences the characteristics of the bending ratcheting behavior slightly after the first cycle.

On the other hand, finite element method is performed for calculating ratcheting strain of straight pipe under load control and vertical displacement control. Bilinear model, Chaboche model, Ohno-Wang model and CJK model are used. It is found that ratcheting strain prediction by Chaboche model is larger than other models. Comparison of experimental results with simulation results is found that ratcheting strain prediction by CJK model is acceptable. It also verifies that the results of load control and displacement control are similar. In addition, load control and displacement control present almost the same ratcheting boundary in the experiment. Moreover, Ratcheting boundary of the simulations has very good correlations with the experiments. Load control can be taken the place of the displacement control and vice versa.

Acknowledgments

The authors gratefully acknowledge financial support for this work from the Fundamental Research Funds for the Central Universities (XNB201501), National Natural Science Foundation of China (No. 51435012, 51471116, 11404054) and Ph.D. Programs Foundation of Ministry of

Education of China (No. 20130032110018).

References

Asada, S., Yamashita, N., Okamoto, A. and Nishiguchi, I. (2002), "Verification of alternative criteria for shakedown evaluation using flat head vessel", *ASME PVP*, **439**, 17-22.

ASME (2007), American Society of Mechanical Engineers, (Section iii), New York, NY, USA.

Bari, S. and Hassan, T. (2000), "Anatomy of coupled constitutive models for ratcheting simulation", *Int. J. Plast.*, **16**(3), 381-409.

Chaboche, J. (1986), "Time-independent constitutive theories for cyclic plasticity", *Int. J. Plast.*, **2**(2), 149-188.

Chaboche, J. (1991), "On some modifications of kinematic hardening to improve the description of ratchetting effects", *Int. J. Plast.*, **7**(7), 661-678.

Chen, X., Jiao, R. and Kim, K.S. (2005), "On the ohno–wang kinematic hardening rules for multiaxial ratcheting modeling of medium carbon steel", *Int. J. Plast.*, **21**(1), 161-184.

Corona, E. (1996), Straight pipe ratcheting data developed at the university of notre dame. [unpublished]

Corona, E. and Kyriakides, S. (1991), "An experimental investigation of the degradation and buckling of circular tubes under cyclic bending and external pressure", *Thin-Wall. Struct.*, **12**(3), 229-263.

Dang-Van, K. and Moumni, Z. (2000), "Evaluation of fatigue-ratcheting damage of a pressurised elbow undergoing damage seismic inputs", *Nucl. Eng. Des.*, **196**(1), 41-50.

DeGrassi, G., Hofmayer, C., Murphy, A., Suzuki, K. and Namita, Y. (2003), "BNL nonlinear pre-test seismic analysis for the NUPEC uitimate strength piping test program", BNL-NUREG-71119-2003-CP.

English, W.F. (1988), "Piping and fitting dynamic reliability program-fourth semi- annual progress report", GE Nuclear Energy, NEDC-31542, November 1986~April 1987..

Gao, B. (2005), "Modeling of material multiaxial ratcheting and ratcheting prediction of pressure piping", Ph.D. Dissertation, Tianjin University of Technology, Tianjin, China. [In Chinese]

Gao, B., Chen, X. and Chen, G. (2006), "Ratchetting and ratchetting boundary study of pressurized straight low carbon steel pipe under reversed bending", *Int. J. Pres. Ves. Pip.*, **83**(2), 96-106.

Guionnet, C. (1989), "Modelization of ratcheting in biaxial experiments", *Nucl. Eng. Des.*, **116**(3), 223-230.

Hassan, T., Zhu, Y. and Matzen, V.C. (1998), "Improved ratcheting analysis of piping components", *Int. J. Pres. Ves. Pip.*, **75**(8), 643-652.

Igari, T., Wada, H. and Ueta, M. (1996), "Plastic buckling and ratcheting of straight pipes subjected to deformation-controlled montonic and cyclic bending", *ASME PVP*, **331**, 47-54.

Isobe, N., Sukekawa, M.a, Nakayama, Y., Date, S., Ohtani, T., Takahashi, Y., Kasahara, N., Shibamoto, H., Nagashima, H. and Inoue, K. (2008), "Clarification of strain limits considering the ratcheting fatigue strength of 316fr steel", *Nucl. Eng. Des.*, **238**(2), 347-352.

Jahanian, S. (1997), "On the incremental growth of mechanical structures subjected to cyclic thermal and mechanical loading", *Int. J. Pres. Ves. Pip.*, **71**(2), 121-127.

Kang, G., Gao, Q. and Yang, X. (2002), "A visco–plastic constitutive model incorporated with cyclic hardening for uniaxial/multiaxial ratcheting of ss304 stainless steel at room temperature", *Mech. Mater.*, **34**(9), 521-531.

Kobayashi, M. and Ohno, N. (2002), "Implementation of cyclic plasticity models based on a general form of kinematic hardening", *Int. J. Numer. Meth. Eng.*, **53**(9), 2217-2238.

Kobayashi, M., Mukai, M. and Takahashi, H. (2003), "Implicit integration and consistent tangent modulus of a time-dependent non-unified constitutive model", *Int. J. Numer. Meth. Eng.*, **58**(10), 1523-1543.

Krämer, D., Krolop, S., Scheffold, A. and Stegmeyer, R. (1997), "Investigations into the ratchetting behaviour of austenitic pipes", *Nucl. Eng. Des.*, **171**(1), 161-172.

KTA, K.A.β. (1995), Sicherheitstechnische regel des kta, komponenten des prima¨rkreises von leichtwasserreaktoren, teil: Auslegung, konstruktion und berchnung, regeladerungsentwurf.

Kulkarni, S., Desai, Y., Kant, T., Reddy, G., Parulekar, Y. and Vaze, K. (2003), "Uniaxial and biaxial

ratchetting study of sa333 gr. 6 steel at room temperature", *Int. J. Pres. Ves. Pip.*, **80**(3), 179-185.
Kulkarni, S., Desai, Y., Kant, T., Reddy, G., Prasad, P., Vaze, K. and Gupta, C. (2004), "Uniaxial and biaxial ratchetting in piping materials—experiments and analysis", *Int. J. Pres. Ves. Pip.*, **81**(7), 609-617.
Ohno, N. and Wang, J.D. (1993a), "Kinematic hardening rules with critical state of dynamic recovery, part i: Formulation and basic features for ratchetting behavior", *Int. J. Plast.*, **9**, 375-390.
Ohno, N. and Wang, J.D. (1993b), "Kinematic hardening rules with critical state of dynamic recovery. Part ii: Application to experiments of ratcheting behavior", *Int. J. Plast.*, **9**, 391-403.
Postberg, B. and Weiß, E. (2007), "Simulation of ratcheting of AISI 316L(N) steel under nonproportional uniaxial loading and high number of load cycles using the Ohno and Wang nonlinear kinematic material model", *Int. J. Pres. Ves. Pip.*, **77**(5), 207-213.
Prager, W. (1956), "A new method of analyzing stresses and strains in work-hardening plastic solids", *J. Appl. Mech.*, **21**(4), 493-496.
Rahman, S.M. (2006), "Finite element analysis and related numerical schemes for ratcheting simulation", Ph.D. Dissertation, North Carolina State University, Raleigh, NC, USA.
Rahman, S.M., Hassan, T. and Corona, E. (2008), "Evaluation of cyclic plasticity models in ratcheting simulation of straight pipes under cyclic bending and steady internal pressure", *Int. J. Plast.*, **24**(10), 1756-1791.
Ranganath, S., Hwang, S. and Tagart, S.W. (1989), "Piping and fitting dynamic reliability program", EPRI Nuclear Power Division.
RCC-MR (2002), Design rules for class 1 equipment rcc-mr codes, revision.
Rider, R.J., Harvey, S.J. and Charles, I.D. (1994), "Ratcheting in pressurized pipes", *Fatigue Fract. Eng. M.*, **17**(4), 497-500.
Scavuzzo, R., Lam, P. and Gau, J. (1991), "Experimental studies of ratcheting of pressurized pipe", *J. Press. Ves. -T. ASME*, **113**(2), 210-218.
Vishnuvardhan, S., Raghava, G., Gandhi, P., Saravanan, M., Pukazhendhi, D., Goyal, S., Arora, P. and Gupta, S.K. (2010), "Fatigue ratcheting studies on tp304 ln stainless steel straight pipes", *Procedia Engineering*, **2**(1), 2209-2218.
Weiß, E., Postberg, B., Nicak, T. and Rudolph, J. (2004), "Simulation of ratcheting and low cycle fatigue", *Int. J. Pres. Ves. Pip.*, **81**(3), 235-242.
Wolters, J., Breitbach, G., Rödig, M. and Nickel, H. (1997), "Investigation of the ratcheting phenomenon for dominating bending loads", *Nucl. Eng. Des.*, **174**(3), 353-363.
Xia, Z., Kujawski, D. and Ellyin, F. (1996), "Effect of mean stress and ratcheting strain on fatigue life of steel", *Int. J. Fatigue*, **18**(5), 335-431.
Yahiaoui, K. and Moffat, D.G. (1996), "Onset of ratcheting in pressurized piping elbows subjected to in-plane bending moments", *Int. J. Pres. Ves. Pip.*, **68**, 73-79.
Yoshida, F., Obataya, Y. and Shiratori, E. (1984), "Mechanical ratcheting behaviors of a steel pipe under combined cyclic axial load and internal pressure", *Society of Materials Science*, *Proceedings of the 27th Japan Congress on Materials Resarch*, Tokyo, Japan, September, pp. 19-23.
Yu, D., Chen, G., Yu, W., Li, D. and Chen, X. (2011), "Visco-plastic constitutive modeling on ohno-wang kinematic hardening rule for uniaxial ratcheting behavior of z2cnd18. 12n steel", *Int. J. Plast.*, **28**, 88-101.
Zakavi, S.J., Zehsaz, M. and Eslami, M.R. (2010), "The ratchetting behavior of pressurized plain pipework subjected to cyclic bending moment with the combined hardening model", *Nucl. Eng. Des.*, **240**(4), 726-737.

CC